Analytical and Bioanalytical Chemistry (2019) 411:5033–5045
https://doi.org/10.1007/s00216-019-01899-8

PAPER IN FOREFRONT

Advancing MS^n spatial resolution and documentation for glycosaminoglycans by sulfate-isotope exchange

Qing Guo[1] · Vernon N. Reinhold[1]

Received: 31 January 2019 / Revised: 29 March 2019 / Accepted: 7 May 2019 / Published online: 1 June 2019

Abstract

Glycosaminoglycans (GAGs) are carbohydrate polyionic polymers that participate in a host of critically important biological processes. A significant difficulty in the comprehensive structural characterization of GAGs is the determination of specific sulfation position isomers. We chose to circumvent sulfate lability by its liberation followed by specific isotope exchange that makes it amenable to methylation, collisional induced dissociation, and MS^n disassembly for a detailed structural characterization. A set of chemistries that include sulfate release, isotopic (CD_3– and CD_3–CO–) replacement, and methylation have been modified to yield a stable product ideal for sequencing by MS^n. Disassembly of these samples provides a detailed read-out of sequence inclusive of all sulfation sites. As documenting steps, we applied these chemical modifications to a series of disaccharides and a synthetic GAG pentamer, Arixtra®. Upon disassembly, glycosidic and cross-ring cleavages define the monomer composition including individual sulfation positions. The N- and O-sulfates are differentiated by deuterium-containing mass compositions. The uronic methylesters do not significantly alter the fragmentation patterns. A fragment library of these products is being assembled as an adjunct to our larger fragment library, some 15 years in the making.

Keywords Glycosaminoglycans · Permethylation · MS^n · Ion trap

Introduction

Glycosylation is one of the most common protein post-translational modifications. Sulfation modifications of glycans play many roles in a diverse range of biological events. Sulfated glycans are related to HIV infection [1], neurological diseases [2], and cancer [3]. Sulfation can be found in various types of glycans, such as N-linked glycans, O-linked glycans, and glycosaminoglycans (GAGs). Both free GAGs and their complexes with proteins are widely known as components of different cells, tissues, and organs. They contribute to a wide variety of biological processes. These linear polysaccharides are highly anionic, widely dispersed with variations in sulfation and hexuronic acid epimerization. The stereochemistry of the hexuronic acid residues of the structure of GAGs is a key feature that affects their interactions with proteins and other biological functions [4–7]. Their acidity and isomeric properties of GAG oligomers make structural characterization challenging.

Heparin is a common GAG and a century has passed since its discovery in 1916, but understanding its fine structure still remains a challenge. Heparan sulfate (HS) shares the basic structure with heparin, differing in the extent of modifications. Most common in heparin, hexuronic acid residues are 2-O-sulfated iduronic acid (IdoA) and glucosamine (GlcN) residues that are sulfated at the N and 6-O positions. HS has a lower degree of sulfation but more variations in sulfation and epimerization within each residue. Recent data suggests that unfractionated heparin (UFH) and low molecular weight heparins (LMWHs), in addition to their anticoagulant activation, also have an anticancer effect [5].

Current preparations of commercial-grade heparin are animal products. The indigenous variabilities as well as animal diets and breed are all reported to have an influence on structural detail [8]. To reduce this natural complexity, samples are frequently depolymerized chemically or enzymatically. These products are then fractionated by combinations of size, charge,

Electronic supplementary material The online version of this article (https://doi.org/10.1007/s00216-019-01899-8) contains supplementary material, which is available to authorized users.

✉ Vernon N. Reinhold
Vernon.Reinhold@unh.edu

[1] The Glycomics Center, Department of Molecular, Cellular, and Biomedical Sciences, University of New Hampshire, Durham, NH 03824, USA

or polarity to LMWHs which are prepared in just this manner. Whether one can show unity in a set of structures remains an open question. Chemical synthesis is considered as an alternative approach for preparing heparin. Arixtra® is an excellent pentasaccharide example that duplicates the natural ATIII binding to heparin. Chemical synthesis of other heparin oligomers is under pursuit.

As a result to the transparency of isomers to mass measurement and the chemical lability of sulfate groups, heparin-related structures remain challenging to characterize. Hexuronic acid introduces epimers (glucuronic acid/iduronic acid) that bring additional structural variability. However, mass spectrometry (MS) and nuclear magnetic resonance (NMR) are both powerful analytical techniques as both are sensitive to subtle structural differences. Instrumental differences are that NMR is more salt tolerant but requires larger sample amounts; purity is essential. Also, it is frequently necessary to have molecular weight and MS fragmentation information for approaching complex samples. In contrast, MS suffers from loss of sulfates during activation analyses and variable positioned counterions introduce further mass variations. Data interpretation from both MS and NMR is most frequently handled by experts.

Tandem mass spectrometry using collisional induced dissociation (CID) produces glycosidic and cross-ring fragmentations that are useful for localizing sites of sulfate groups in GAG oligosaccharides. The fragmentation pattern of GAGs using CID-MS/MS is dependent on the charge state of the molecular ion and the ions pairing the sulfate negative charge [9]. However, loss of sulfates accompanies many peaks and complicates the resulting tandem mass spectra. The higher charge state of the molecular ions has shown improvement for minimizing sulfate loss, in the meantime, maximizing glycosidic bond cleavages [9, 10]. In addition, CID preferably breaks the most labile glycosidic bonds; therefore, the structural information is often limited by only performing a single-stage fragmentation. However, the charge–charge repulsion limits the ability to achieve a higher charge state that can produce sufficient intensity for CID-MS/MS. In addition, epimer-specific fragments [11] produced by tandem mass spectrometry of native GAG oligosaccharides have been studied intensively, as well as a fully synthetic pentasaccharide Arixtra [12]. Exchanging H^+ with metal cations such as Na^+ or Ca^{2+} has been shown to stabilize sulfate groups and enhance the formation of more structurally informative ions [9, 11–14]. Structures as well as abundance measurements of B and Y fragment ions are often resolved by statistical methods [15], but most CID studies appear to have utilized too high energy and short reaction times before mass extraction and measurement, resulting in abundant B and Y fragments. Such conditions fail to allow the critical time required to form cross-ring fragments that make up the isomeric linkage ions. To further make tandem mass spectrometry effective for structural characterization of GAGs, other fragmentation methods such as electron detachment dissociation (EDD) [16–19] and electron transfer dissociation (ETD) [20–22] have been applied to generate more glycosidic as well as cross-ring cleavages to identify the location of sulfate groups. Such operating parameters show promise for detailed structural information on native GAG oligomers; however, prudent selection of precursor ions and statistical comparison of fragment ions suggests critical challenges for de novo structural elucidation.

Hyphenated MS^n-based methods, such as LC-MS^n, offer an approach with considerable information to understand sulfation patterns and uronic acid epimerization [23–26]. In addition, capillary electrophoresis mass spectrometry (CE-MS)-based separation using negative mode electrospray ionization provides shorter time and higher resolution for heparin oligosaccharides [27]. Ion mobility mass spectrometry in combination with MS^n has been used for isomer separation and structural characterization of chondroitin sulfate oligosaccharides [28]. Most recently, MS^n has been coupled to infrared ion spectroscopy to distinguish GalNAc4S and GalNAc6S [29]. As GAG chain length increases, the subtle differences in sulfation isomers are difficult to separate using liquid chromatography. Attempts to improve peak resolution with different chemical derivatizations result in variations in retention times and mass spectral patterns. This makes it unlikely for instrument-independent data sharing between labs. A universal protocol capable of detailing subtle structures would be in high demand.

The permethylation step improves and enhances MS ionization and fragmentation. Methylation prior to analysis leads to increases in signal and cross-ring cleavages upon collisional disassembly. Activation of permethylated ions by gas collisions and detailing products by repetitive steps (MS^n) of disassembly provides innate control that introduces a sequencing strategy most successful for glycans of proteins and lipids [30–35]. The application of this technology to GAGs would be expected to proceed along comparable lines providing disassembled products suitable to consider reversibly as a sequence technology. MS^n creates a tractable pathway to pursue these structural details and has been successfully applied for the determination of structural isomers of N-linked and O-linked glycans [33–37]. The complexity of GAG structures includes intact chain composition, oligosaccharide composition, disaccharide composition, and uronic acid composition. For a number of years, we have shown ion trap mass

spectrometry to be the most effective MS strategy for precision sequencing of oligosaccharide structures. It is controlled by indigenous chemical disassembly and the MS^n fragmentation pattern is instrument platform independent and highly reproducible. In our extensive experience, variation of collision energy in CID does not affect the relative intensity among product ions. This leads to establishment of a documented MS^n library of mass spectra generated from known structures. Spectra matching compares user-generated CID mass spectrum to previously collected mass spectral data in the library. This tool enables outside users who do not have the expertise to easily apply MS^n for glycan sequencing and structure determination.

To adapt MS^n for GAG sequencing, a universal method is needed to supply structural information of monosaccharide composition in terms of uronic acid epimerization, N-glucosamine and O-sulfation pattern, and the sequence of these residues along the chains. The present work introduces a series of selective chemical steps that includes sulfate release, isotopic (CD_3– and CD_3–CO–) replacement, and methylation that yields a stable product ideal for sequencing by MS^n. Resulting MS^n fragmentation patterns have proven to be independent of instrument platform and isotopic label modification. Given the wide availability of ion-trap instruments and the growing number of glycoanalysts who permethylate their samples, this would have great benefit to the application of MS^n between various glycomics facilities by data sharing rather than each facility building their own libraries.

Materials and methods

Materials

Heparin/heparan sulfate disaccharide standards were purchased from V-laboratories, Inc. (Covington, LA, USA) and were used without further purification. Unsaturated heparin/heparan sulfate disaccharide standards are produced from enzymatic digestion and sold in the form of their sodium salts. D2A0 is the minor product of the action of heparinase II on heparin. D0A6 is the product of the action of heparinases II and III on heparin and heparin sulfate.

Arixtra®, fondaparinux sodium, was produced by GlaxoSmithKline (Brentford, Middlesex, UK). PD MidiTrap G-10 desalting columns were purchased from GE healthcare (Piscataway, NJ, USA). All other reagents were from Sigma-Aldrich (Milwaukee, WI, USA). C_{18} Sep-Pak cartridges were from Waters (Franklin, MA, USA). For convenience, Arixtra® is abbreviated as Arixtra in the text [38].

Desalting

Arixtra contains around 23 mg sodium salts in 0.5 mL solution of each dose. Conversion of this sample to its triethylammonium (TEA) salt is not very efficient owing to the high sodium content. Incomplete conversion of TEA salts will reduce its solubility in dimethyl sulfoxide (DMSO), thus affecting following sample preparation steps. Therefore, a desalting step is added to clean up the sample prior to ion exchange.

PD MidiTrap G-10 columns are pre-packed with Sephadex G-10, which is a gel filtration medium prepared by crosslinking dextran with epichlorohydrin. Sephadex G-10 has an exclusion limit of greater than 700 molecular weight. Because its separation mechanism is based on size differences, any species have a molecular weight smaller than 700 will be retained in the column. Fluid flow through the column was accomplished using gravity only. Water was used as equilibration buffer. The column was equilibrated with 20 mL water. The flow-through was discarded. Then, 0.4 mL of 1 mg/mL Arixtra was applied to the column. Water was added to reach a total volume of 1.6 mL. The flow-through was collected as the first flow. Then Arixtra was eluted with 1.6 mL water and collected as the second flow or sample flow. All the flow-through was lyophilized [38].

Chemical derivatization

Permethylation with methyl iodide

Heparin/heparan sulfate disaccharides The heparin disaccharides were permethylated using methyl iodide following the method described by Heiss et al. [39] without further modification.

Synthetic heparin pentasaccharide, Arixtra To increase its solubility in DMSO, the desalted Arixtra was passed through a self-packed cation-exchange column with Dowex 50Wx8 resin to generate TEA salts. The dried TEA salts were completely dissolved in 400 μL of DMSO and 400 μL of anhydrous suspension of 200 μg/μL sodium hydroxide in DSMO [40], followed by 400 μL of iodomethane. The permethylation was performed at room temperature by vortex for 5 min and then sonication for 25 min. The reaction was quenched by adding 2 mL of ion pairing buffer (100 mM triethylamine, pH adjusted to 7 with conc. acetic acid).

The reaction mixture was sparged with nitrogen to remove excess iodomethane before G-10 column cleanup. Equilibration buffer was 30% acetonitrile/water. The column was equilibrated with 20 mL buffer. The flow-through was discarded. The dried reaction mixture was re-suspended in 600 μL 30% acetonitrile/water. Then the solution was applied to the column. Equilibration buffer was added to reach a total volume of 1.5 mL. The flow-through was collected as the first

flow. Then permethylated Arixtra was eluted with 1.7 mL equilibration buffer and collected as the second flow or sample flow. The sample flow was lyophilized.

Solvolytic desulfation

The dried permethylated product was completely dissolved in 400 μL of 50% methanol/water, then loaded onto a cation-exchange column in H^+ form. The IE column was flushed with 5 mL of 50% methanol/water, then 1 mL pyridine was added to the solution, followed by lyophilization.

The dried pyridinium salts were re-suspended in 100 μL of 10% methanol/DMSO and incubated at 100 °C for 6 h to remove the sulfates [41], followed by lyophilization.

N-Acetylation with acetic anhydride-d_6

The dried desulfated product was re-suspended in 500 μL of ammonium carbonate in 30% acetonitrile/water and 1250 μL of acetic anhydride or acetic anhydride-d_6, and incubated at room temperature overnight, followed by lyophilization [42]. This step was intended to prevent formation of a permanent positive charge on free glucosamine (generated from desulfation) during the 2nd permethylation step.

Permethylation with deutero methyl iodide

The 2nd permethylation was performed using a spin column procedure, but instead of iodomethane, iodomethane-d_3 was used to replace acetyl groups on O-sulfates. A spin column (Harvard Apparatus) was packed with sodium hydroxide beads to about 3 cm depth. The packed column was rinsed with acetonitrile once, then DMSO twice. Sample was dissolved in 141.6 μL DMSO, 52.8 μL iodomethane-d_3, and 0.9 μL water. Then the mixture was applied to the column to react for 15 min. The reaction mixture was collected by spinning the column at 2000 rpm for 2 min. Then, 70 μL DMSO and 26 μL iodomethane-d_3 were added to the sample tube, and transferred to the spin column. The column was spun at 2000 rpm for 2 min to collect all sample. After that, 60 μL iodomethane-d_3 was added to the reaction mixture and re-applied to the column to repeat the reaction for another 15 min. After reaction, the total reaction mixture was collected by spinning the column at 4000 rpm for 2 min. The mixture was transferred to a test tube containing one aliquot of chloroform and one aliquot of 10% acetic acid/water. At least five water washes of the sample layer (organic layer) were performed during the liquid–liquid extraction cleanup. The sample layer was dried for later ESI-IT-MS^n analysis [38].

Glycan analysis

The fully derivatized Arixtra was cleaned up with RP-LC/MS. Reversed-phase liquid chromatography (RPLC) was performed on a Thermo VelosPro mass spectrometer with a Thermo Surveyor MS pump and Thermo Surveyor autosampler. Separation was carried out on a BDS HYPERSIL C_{18} column (Thermo), 2.1 mm × 150 mm, 3 μm. Mobile phase A was 25 μM sodium acetate prepared with HPLC-grade water. Mobile phase B was acetonitrile. A linear gradient of mobile phase B from 25% to 55% over 36 min was used, with a flow rate of 200 μL/min. Online positive ion MS profiles were obtained from a VelosPro (Thermo Fisher Scientific, Waltham, MA) equipped with an electrospray ion source. The capillary temperature was 375 °C. The collision energy was set as 35% normalized collision energy.

Fractions collected from RP-LC/MS were dissolved in 50% (v/v) methanol/water before direct infusion analysis on a Thermo LTQ or Thermo VelosPro equipped with a TriVersa Nanomate nanoelectrospray ion source (Advion, Ithaca, NY). MS^n spectra were obtained from this chip-based nanoESI interface by direct infusion ESI ion trapping.

MS^n spectra were obtained with either Thermo LTQ or VelosPro equipped with a nanospray ESI source (Thermo Fisher Scientific, Waltham, MA). Details are noted in specific figures.

Results and discussion

Resolving isomeric structures for heparin disaccharides

D2A0 and D0A6 are heparin-derived disaccharide standards. They are structural isomers. D2A0 has 2-O-sulfation at unsaturated uronic acid (ΔUA) residues while D0A6 has 6-O-sulfation at glucosamine (GlcN) residues. After chemical derivatization, all available protons are exchanged with methyl groups and sulfo groups are converted to methyl-d_3 groups. With this isotopic label, sulfated disaccharide derivatives weigh 3 Da heavier than non-sulfated disaccharide derivatives.

At MS^3 level (*m/z* 506–359), fragments at *m/z* 255, *m/z* 271, and *m/z* 285 (Fig. 1b) are 3 Da heavier than fragments at *m/z* 252, *m/z* 268, and *m/z* 282, respectively (Fig. 1a). This 3-Da mass difference indicates that D0A6 has a sulfation at the GlcN residue. As a consequence of observing fragments at *m/z* 285 and *m/z* 255, this sulfation is at the 6-O position.

In the meantime, there is no sulfation at the GlcN residue of D2A0. At the MS^3 level, fragments at *m/z* 255, *m/z* 271, and *m/z* 285 (Fig. 1b) and fragments at *m/z* 252, *m/z* 268, and *m/z* 282 (Fig. 1a) are generated from the same parent ion at *m/z* 359. Therefore, the sulfo group of D2A0 is at the 2-O position of the unsaturated ΔUA residue.

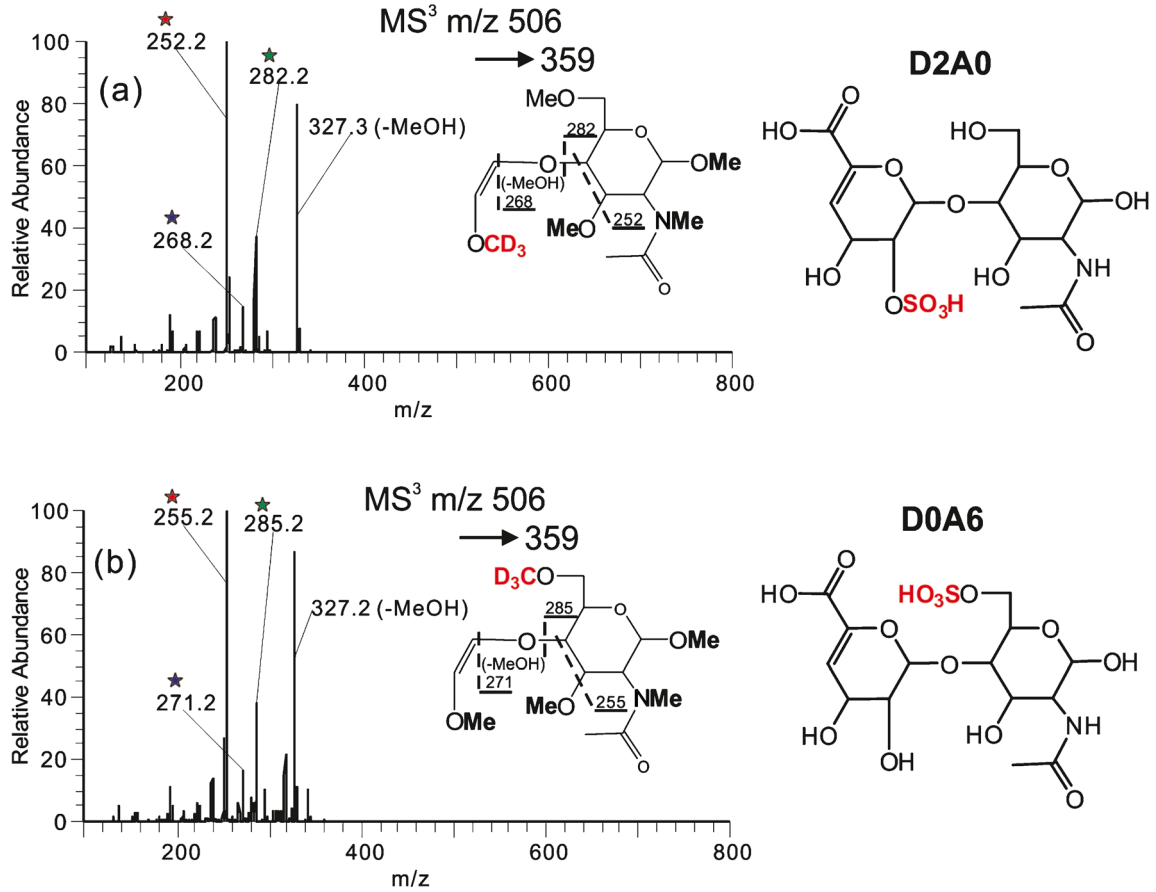

Fig. 1 A simple identification of isomeric structures using MS^n Analysis. Spectra were acquired by Thermo LTQ. Native unsaturated heparin disaccharide standards (D2A0 and D0A6) were chemically derivatized to convert O-sulfates to O-CD_3 groups. **a** MS^3 spectra of derivatized D2A0. **b** MS^3 spectra of derivatized D0A6

Chemical derivatization of synthetic heparin pentasaccharide, Arixtra

Isotopic replacement of N- and O-sulfates

As a key point of adapting GAGs to MS^n analysis, isotopic (CD_3– and CD_3–CO–) replacement provided mass shifts to label the sulfation positions. As shown in Fig. 2, all available protons were exchanged with methyl groups by performing permethylation with methyl iodide. This permethylation was named as 1st permethylation. To distinguish the sulfation position from non-sulfation position, particularly for O-sulfates, all the sulfates have been removed by solvolytic desulfation. After derivatization, N-sulfates were converted to N-acetyl groups (CD_3–CO–N–R) while O-sulfates were converted to methyl esters (CD_3–O–R). With this specific isotopic replacement, sulfation sites have been localized for MS^n analysis.

As an important component of derivatization, permethylation contributes significantly to MS-based structural analysis. However, permethylation of sulfated glycans are very difficult because of the insolubility of very polar glycans in DMSO. Arixtra is a highly sulfated synthetic pentasaccharide. To make it soluble, desalted Arixtra was passed through a cation exchange column to generate its TEA salts [43]. This effort is remarkable for initiation of the derivatization process. The 1st permethylation was performed using a modified protocol from heparin disaccharide standards [39]. The completeness of permethylation is related to many factors, such as solubility in DMSO, NaOH concentration in DMSO, quenching solution, and reaction time. Upon investigation, the best conditions are summarized in the sample preparation section. After the reaction, the mixture was cleaned up using the G-10 desalting column (molecular weight cutoff of 700 Da) instead of a C_{18} column to get maximum recovery of both complete and incomplete permethylation products.

After the 1st permethylation, non-sulfation positions were masked with methyl groups except where a sulfated amine residue contains a 3-O-sulfate. An undermethylation site was found at sulfated glucosamine residues containing 3-O-sulfation with Arixtra. This phenomenon is consistent with previous studies of permethylated Arixtra-like oligomers [12] and NMR

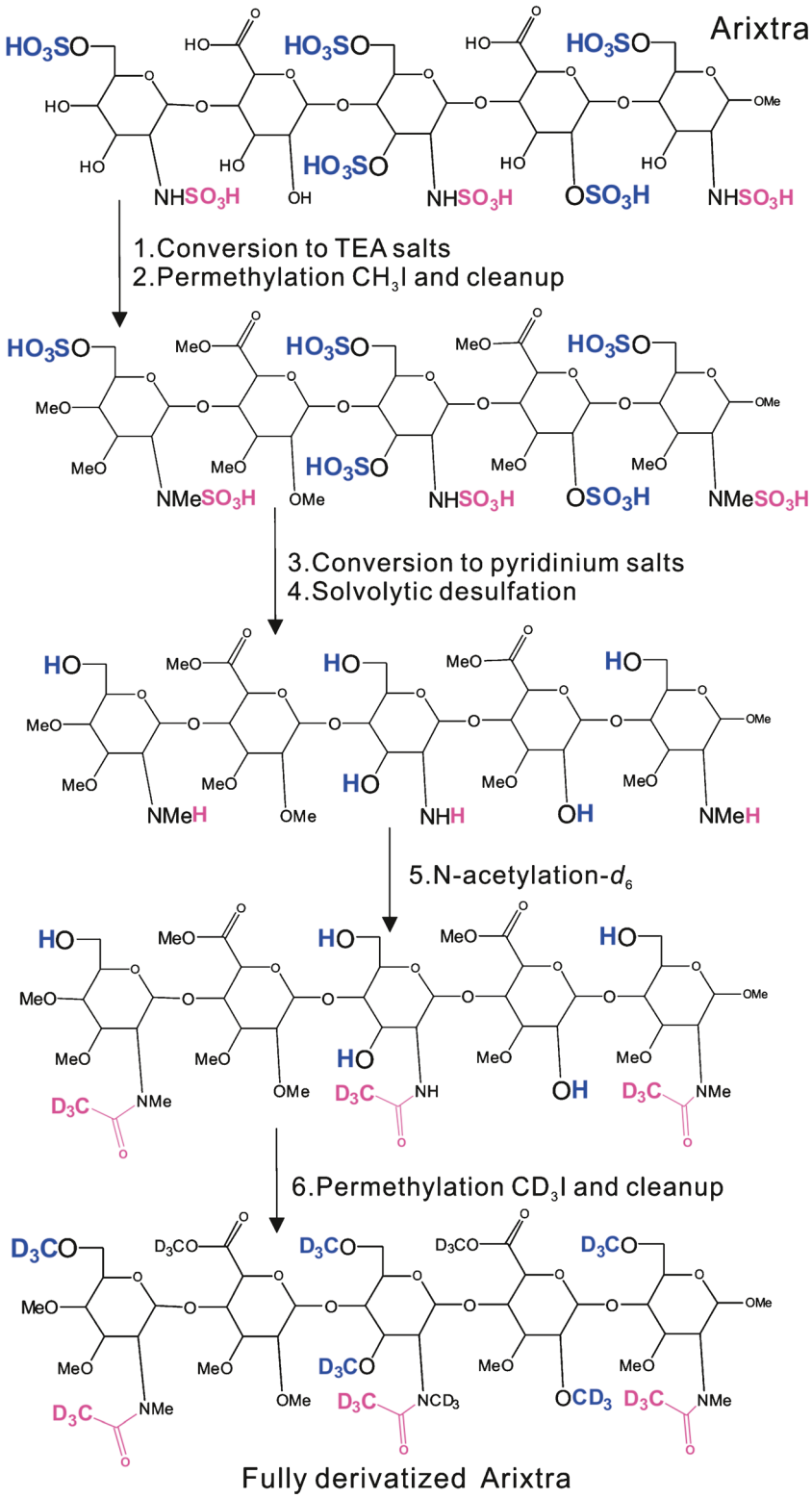

Fig. 2 Experimental workflow adapting GAGs to MS^n analysis. To enhance DMSO solubility, the sample was passed through a cation exchange column to prepare the TEA salt, followed by CH_3I methylation. After removal of sulfates, N-acetylation, and CD_3I remethylation, the N-sulfates were converted to CD_3–CO–N groups and O-sulfates were converted to O-CD_3 groups

studies of Arixtra [44]. The position of the undermethylation site was followed up after desulfation, via acetylation as well as deutero permethylation. The traceable mass shift after each derivatization step confirmed the presence of one undermethylated position. MS^n analysis was performed to locate the underpermethylation site. Another problem found with permethylation was saponification of uronic acids. Owing to the presence of NaOH, permethylation was performed under strongly basic conditions. Arixtra has two

uronic acid residues; thus, saponification of carboxyl esters happened when the pH is basic. As the acidity of quenching solution increased, saponification side products were gradually reduced. Other possible side products are summarized in ESM Table S3 and Fig. S1.

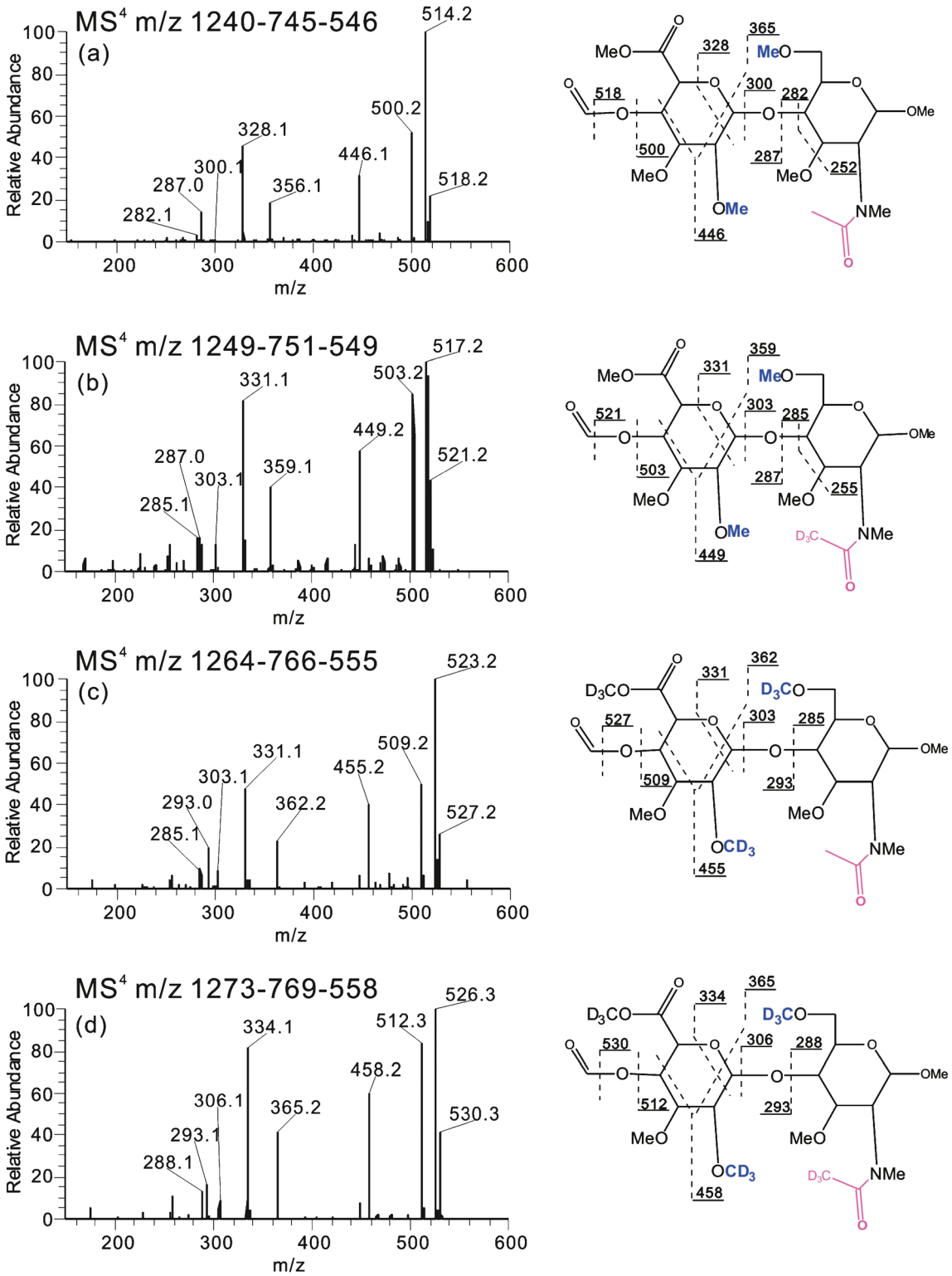

Fig. 3 Identification of sulfation sites. **a** No isotopic label, MS^4 *m/z* 1240–745–546; **b** Isotopic label on N-sulfates, MS^4 *m/z* 1249–751–549; **c** Isotopic label on O-sulfates, MS^4 *m/z* 1264–766–555; **d** Isotopic label on O- and N-sulfates, MS^4 *m/z* 1273–769–558. Spectra were acquired by Thermo VelosPro

After permethylation, sulfo groups were chemically released by solvolytic desulfation. Permethylated Arixtra was converted to its pyridinium salt before solvolysis. Incomplete desulfation was found at the 3-O position or 2-O-sulfoiduronic acid (ESM Fig. S3).

After release of sulfates, Arixtra was acetylated with acetic anhydride-d_6. This step served two purposes: to label the N-sulfated position and to prevent formation of a permanent positive charge on the free amino group in the next permethylation step. N-sulfates have been replaced by N-deutero acetyl groups. The 2nd permethylation was carried out in a spin column with methyl iodide-d_3 to label O-sulfated positions. This second methylation step is critical for CID-MS^n disassembly. In the process of acetylation, the free hydroxyl groups produced by liberation of O-sulfates were partially acetylated under the conditions of N-acetylation. Complete acetylation of all sulfo groups is achievable under more harsh conditions, which is desirable for reversed-phase chromatography to get better separation of isomeric structures. However, the O-acetyl bond is very labile and cleaved easily during CID (shown in ESM Fig. S6). And the position of loss is not predictable. This significantly hinders the adoption of MS^n for identification of sulfation positions. Therefore, the follow-up methylation step to replace O-acetyl with a more stable O-methyl is necessary to generate reproducible MS^n fragmentation. After derivatization, sulfation positions were replaced with isotopically labeled sites, followed by multistage spatial disassembly to reveal all structural details.

Yield estimation of Arixtra is particularly challenging as a result of the absence of a chromophore. Before removal of sulfates, the yield (ion exchange with TEA and permethylation) was estimated on the basis of peak area of total ion chromatogram (TIC) of ion pairing reversed-phase liquid chromatography coupled with mass spectrometry (IP-RP-LC/MS). Using peak area of TIC is considered a semi-quantitative way to calculate the yield. In this case, Arixtra or permethylated Arixtra was not detected as a single molecular ion. Its MS profile comprised various adducts of ion pairing agent and sulfate loss products (shown in ESM Fig. S1). A major side product of permethylation was an elimination of O-sulfate. The yield before desulfation was estimated to be less than 50%. After removal of sulfates, the yield was estimated on th basis of relative peak abundance. Yield of solvolytic desulfation was estimated to be less than 60% (shown in ESM Fig. S7). The overall yield of this derivatization protocol was estimated to be less than 30% considering these two major side reactions.

If the fully derivatized product ion is observable in MS profile, inevitable sample loss during each step is acceptable for MS^n structural analysis.

Identification of sulfation sites

To verify sulfation positions, different combinations of isotopic labels were applied to Arixtra in chemical derivatization processes, including two permethylation steps. The first permethylation step was to block non-sulfated positions; the second permethylation was to label O-sulfate positions. In addition, N-sulfates were labeled using acetic anhydride-d_6 during N-acetylation. At MS^4 level, fragment ion at *m/z* 287 was observed in both Fig. 3a and b. This ion indicated that only the N-sulfo group was isotopically labeled. From Fig. 3a to b, the rest of fragment ions were shifted by 3 Da. This verified that only one N-sulfo group was present in the precursor ion. As an example, fragment ion at *m/z* 285 in Fig. 3b was 3 Da heavier than fragment ion at *m/z* 282 in Fig. 3a. This was used to confirm that N-sulfation was present at the rightmost monosaccharide sequence. Note that when performing the second permethylation with methyl iodide-d_3, transesterification was observed at uronic acids. Consequently, one additional deutero methyl group was found at the uronic acid position. However, the uronic methyl esters did not significantly alter the fragmentation patterns. Comparing to Fig. 3a, fragment ion at *m/z* 293 was 6 Da heavier than the ion at *m/z* 287 in Fig. 3c, corresponding to two isotopic labels. Comparing to fragment ions at *m/z* 331 and *m/z* 449 of Fig. 3b, fragment ions from cross-ring cleavage (*m/z* 331 and *m/z* 455) confirmed that one isotopic label was on a uronic methyl ester and the other one was at the 2-O position. When all the sulfation positions were labeled as seen in Fig. 3d, fragment ion at *m/z* 288 verified 6-O-sulfation.

MS^n structural details of Arixtra

Positive MS^n spectra were obtained from the VelosPro equipped with TriVersa Nanomate Advion. After removal of sulfates, Arixtra was acetylated with acetic anhydride-d_6, then permethylated with CD_3I. Positive MS^n analyses were performed to fully derivatized Arixtra (profiles were included in ESM Fig. S4). At MS^2 level (Fig. 4a), the molecule broke into two parts as a result of glycosidic bond cleavage between saccharide #2 and #3. C_2 and Z_2, B_3 and Y_3 ions represented fragments

Fig. 4 Identification of Arixtra sulfation patterns, MS^n details. After removal of sulfates, Arixtra was acetylated with acetic anhydride-d_6, then remethylated with CD_3I. Positive MS^n analyses were performed to fully derivatized Arixtra. **a** MS^2 *m/z* 1273; **b** MS^3 *m/z* 1273–766; **c** MS^4 *m/z* 1273–766–527; **d** MS^3 *m/z* 1273–530. Spectra were acquired on Thermo VelosPro

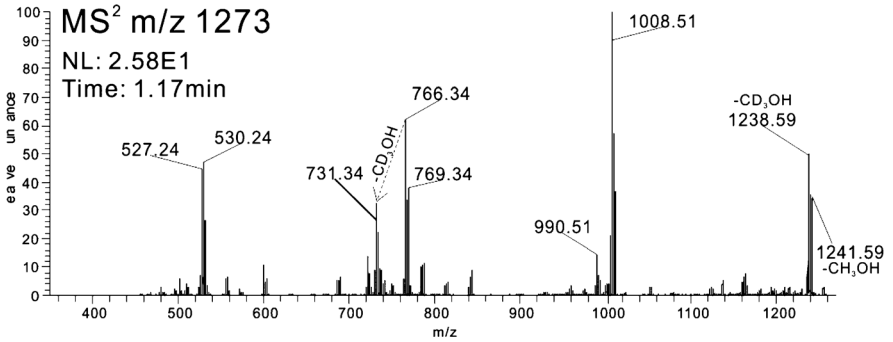
MS^2 m/z 1273
NL: 2.58E1
Time: 1.17min
1008.51
766.34
-CD$_3$OH
1238.59
527.24
530.24
731.34
769.34
990.51
1241.59
-CH$_3$OH
m/z

(a)

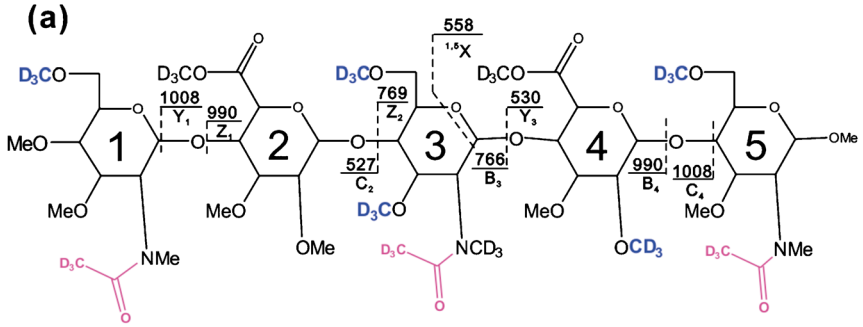
558
1,5X
1008
Y$_1$
990
Z$_1$
769
Z$_2$
530
Y$_3$
527
C$_2$
766
B$_3$
990
B$_4$
1008
C$_4$
1
2
3
4
5
MeO
OMe
NMe
NCD$_3$
OCD$_3$

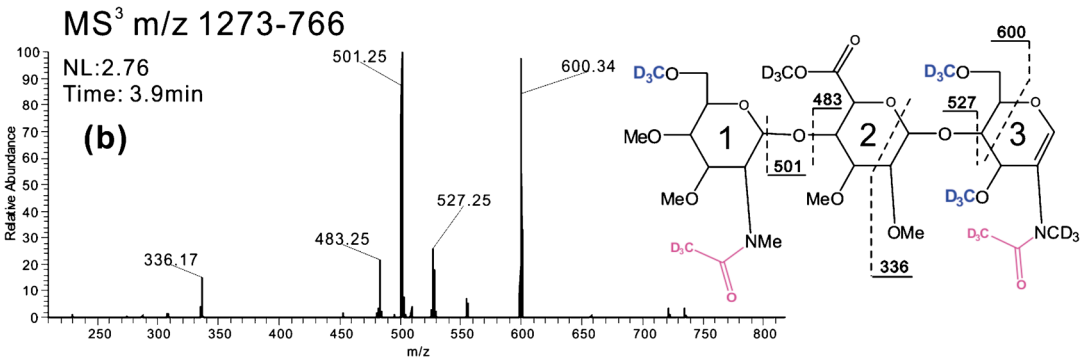
MS^3 m/z 1273-766
NL:2.76
Time: 3.9min
(b)
501.25
600.34
527.25
483.25
336.17
Relative Abundance
m/z
600
483
527
501
336

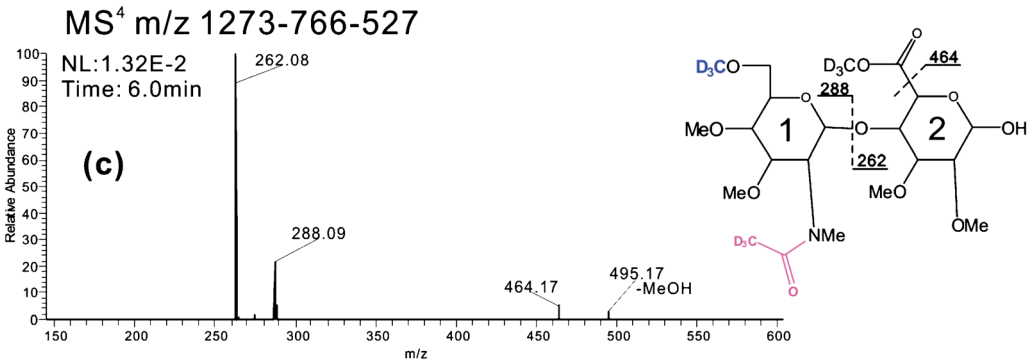
MS^4 m/z 1273-766-527
NL:1.32E-2
Time: 6.0min
(c)
262.08
288.09
464.17
495.17
-MeOH
Relative Abundance
m/z
464
288
262
OH

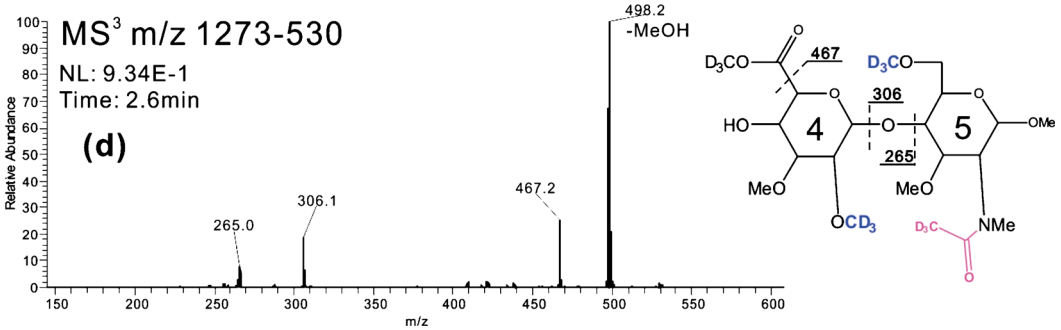
MS^3 m/z 1273-530
NL: 9.34E-1
Time: 2.6min
(d)
498.2
-MeOH
467.2
306.1
265.0
Relative Abundance
m/z
467
306
265
HO
4
5

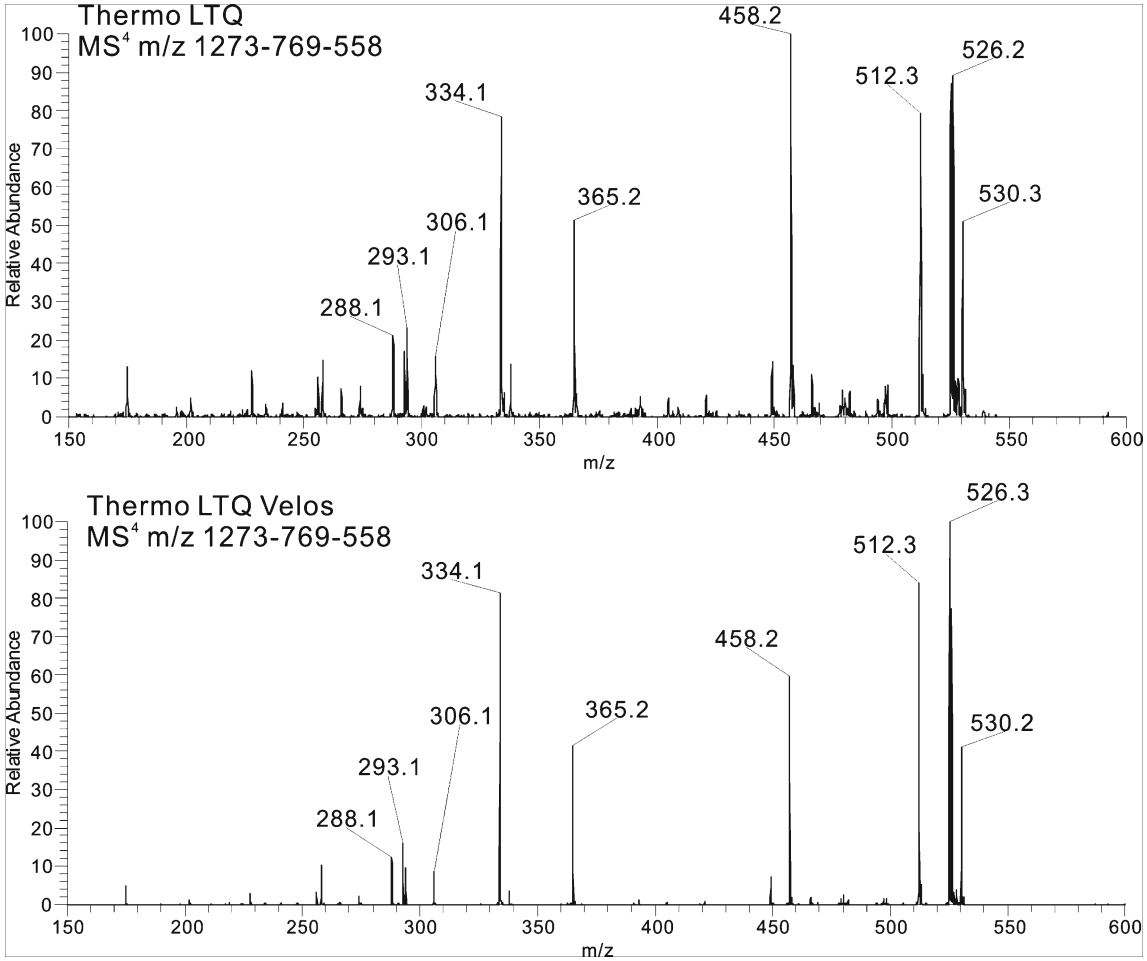

Fig. 5 Spectra fidelity at MS^4 level for fully derivatized Arixtra, Thermo LTQ/Thermo VelosPro

from glycosidic bond cleavages. At MS^3 level (Fig. 4b) of B_3 ion at *m/z* 766, glycosidic cleavage between glucuronic acid residue #2 and GlcNS residue #1 resulted in fragments at *m/z* 501 and *m/z* 483. C_3 ion at *m/z* 527 was the glycosidic cleavage between glucuronic acid residue #2 and 3-O-sulfated GlcNS residue #3. Another dominant fragment ion at *m/z* 600 was the 3,5-cross-ring cleavage at the 3-O-sulfated GlcNS residue #3. The other cross-ring cleavage resulted in fragment at *m/z* 336, which was the 3,5-cross-ring cleavage at glucuronic acid residue #2. In MS^4 (Fig. 4c) of C_3 ion at *m/z* 527, fragment ions at *m/z* 262 and *m/z* 288 were the glycosidic cleavages between glucuronic acid residue #2 and GlcNS residue #1. Loss of deuterated carboxylic acid group glucuronic acid residue #2 and one MeOH resulted in fragments at *m/z* 464 and *m/z* 495, respectively. At MS^3 level (Fig. 4d) of Y_3 ion at *m/z* 530, fragment ions at *m/z* 306 and *m/z* 265 were the glycosidic cleavages between iduronic acid residue#4 and GlcNS residue #5. Loss of deuterated carboxylic acid group at iduronic acid residue#4 and one MeOH resulted in fragments at *m/z* 467 and *m/z* 498, respectively. In MS^4 spectrum (Fig. 4c) of C_3 ion at *m/z* 527, fragment ion at *m/z* 288 suggested that there was one sulfo group at the 6-O-position of GlcNS residue #1. Fragment ions at *m/z* 336 and *m/z* 600 at MS^3 level of B_3 ion at *m/z* 766 indicated 3-O-sulfation and 6-O-sulfation of the GlcNS residue #3, respectively. Fragment ion at *m/z* 265 at MS^3 level of Y_3 ion at *m/z* 530 suggested that one sulfo group was present at the 2-O position of the iduronic acid residue #4. In the meantime, fragment ion at *m/z* 306 suggested that 6-O-sulfation was present at GlcNS residue #1.

Spectral fidelity was observed with all sample types in a large cross selection of samples run under comparable conditions, including synthetic and natural samples and even MS^2 in triple quadrupoles. In this study, spectra were acquired by Thermo LTQ and Thermo VelosPro. As shown in Fig. 5, the fragmentation pattern was very similar between the two ion traps. This favorable comparison suggests that the documentation of the spectra can support analysis on a large number of instruments currently in use.

Conclusion

For several years, we have shown that the sequential mass spectrometry strategy is the most effective at directly unraveling linkage isomeric fragments, (C_1–O–C_X, where C_X would include a C_2, C_3, C_4, or a C_6 carbon). Stepwise MS^n disassembly is initiated by gas-phase collisional activation and the outcome fragmentation is defined by innate structural features of precursor ions explained by basic organic chemistry. We have been collecting these spectra in a searchable file with the goal of facilitating greater collaborative interactions, a fundamental component for advancing glycosylation research.

Unlike those N- and O-linked glycoprotein glycans with various linkages, structural characterization of GAGs mainly encounters difficulty in determination of specific sulfation position isomers. The goal of this derivatization protocol is to utilize the advantages of permethylation and sequential mass spectrometry to provide a novel approach for GAG structural analysis. We describe here a set of chemistries that specifically replaces sulfate residues with a stable isotopic analog that makes it amenable to methylation, CID, and MS^n disassembly for a detailed structural characterization. After derivatization, O-sulfates were converted to O-CD_3 groups and N-sulfates were converted to N-deutero acetyl groups. Although acetylation may not be a necessary step, as a general approach of identifying sulfation position, acetylation should be included considering the presence of N-sulfates.

There is an additional attachment of deuteron methyl groups at uronic acid residues after detero permethylation. Under strong basic conditions, transesterification happens at the carboxyl position which held a methyl ester. On the basis of our extensive experience with permethylated heparin disaccharide standards, this methyl ester is always converted to deutero methyl ester. By only adjusting pH after deutero permethylation, this reaction goes to completion.

The protocol has been tested and modified using a highly sulfated heparin pentasaccharide (Arixtra). Given an unusual feature of Arixtra's synthetic structure, an underpermethylation site was found at sulfated glucosamine residues containing a 3-O-sulfation. As mentioned earlier, MS^n fragmentation is controlled by indigenous chemical disassembly. Hence, neither uronic methyl esters nor additional N-deutero acetyl groups would significantly alter the fragmentation patterns. In addition, MS^n fragmentation pattern is instrument platform independent. In this case, the same precursor ion has shown very similar MS^n fragmentation pattern in both Thermo LTQ and VelosPro ion trap instruments.

For the purpose of de novo structural analysis, a long-term goal of this work is to document suitable CID spectra from dual permethylated GAG oligosaccharides. This would be an addition to our current mass spectral library.

Acknowledgements This work was supported by National Cancer Institute of National Institutes of Health (USA) through the Common Fund of Glycoscience (U01CA221215).

Compliance with ethical standards

Conflict of interest The authors declare that they have no conflict of interest.

References

1. Pomin VH, Bezerra FF, Soares PAG. Sulfated glycans in HIV infection and therapy. Curr Pharm Des. 2017;23(23):3405–14. https://doi.org/10.2174/1381612823666170127113958.
2. Kadomatsu K, Sakamoto K. Sulfated glycans in network rewiring and plasticity after neuronal injuries. Neurosci Res. 2014;78:50–4. https://doi.org/10.1016/j.neures.2013.10.005.
3. Varki A, Kannagi R, Toole BP. Glycosylation changes in cancer. New York: Cold Spring Harbor Laboratory Press; 2009.
4. Pellegrini L. Role of heparan sulfate in fibroblast growth factor signalling: a structural view. Curr Opin Struct Biol. 2001;11(5):629–34. https://doi.org/10.1016/S0959-440X(00)00258-X.
5. Afratis NA, Karamanou K, Piperigkou Z, Vynios DH, Theocharis AD. The role of heparins and nano-heparins as therapeutic tool in breast cancer. Glycoconj J. 2017;34(3):299–307. https://doi.org/10.1007/s10719-016-9742-7.
6. Afratis N, Gialeli C, Nikitovic D, Tsegenidis T, Karousou E, Theocharis AD, et al. Glycosaminoglycans: key players in cancer cell biology and treatment. FEBS J. 2012;279(7):1177–97. https://doi.org/10.1111/j.1742-4658.2012.08529.x.
7. Kreuger J, Spillmann D, Li J-p, Lindahl U. Interactions between heparan sulfate and proteins: the concept of specificity. J Cell Biol. 2006;174(3):323–7. https://doi.org/10.1083/jcb.200604035.
8. Zhang F, Yang B, Ly M, Solakyildirim K, Xiao Z, Wang Z, et al. Structural characterization of heparins from different commercial sources. Anal Bioanal Chem. 2011;401(9):2793–803. https://doi.org/10.1007/s00216-011-5367-7.
9. Zaia J, Costello CE. Tandem mass spectrometry of sulfated heparin-like glycosaminoglycan oligosaccharides. Anal Chem. 2003;75(10):2445–55. https://doi.org/10.1021/ac0263418.
10. Naggar EF, Costello CE, Zaia J. Competing fragmentation processes in tandem mass spectra of heparin-like glycosaminoglycans. J Am Soc Mass Spectrom. 2004;15(11):1534–44. https://doi.org/10.1016/j.jasms.2004.06.019.
11. Kailemia MJ, Patel AB, Johnson DT, Li L, Linhardt RJ, Amster IJ. Differentiating chondroitin sulfate glycosaminoglycans using collision-induced dissociation; uronic acid cross-ring diagnostic fragments in a single stage of tandem mass spectrometry. Eur J Mass Spectrom. 2015;21(3):275–85. https://doi.org/10.1255/ejms.1366.
12. Kailemia MJ, Li L, Ly M, Linhardt RJ, Amster IJ. Complete mass spectral characterization of a synthetic ultralow-molecular-weight heparin using collision-induced dissociation. Anal Chem. 2012;84(13):5475–8. https://doi.org/10.1021/ac3015824.
13. Taylor CJ, Burke RM, Wu B, Panja S, Nielsen SB, Dessent CEH. Structural characterization of negatively charged glycosaminoglycans using high-energy (50–150 keV) collisional activation. Int J Mass Spectrom. 2009;285(1–2):70–7. https://doi.org/10.1016/j.ijms.2009.04.009.
14. Kailemia MJ, Li L, Xu Y, Liu J, Linhardt RJ, Amster IJ. Structurally informative tandem mass spectrometry of highly sulfated natural and chemoenzymatically synthesized heparin and heparan sulfate

glycosaminoglycans. Mol Cell Proteomics. 2013;12(4):979–90. https://doi.org/10.1074/mcp.M112.026880.
15. Bielik AM, Zaia J. Multistage tandem mass spectrometry of chondroitin sulfate and dermatan sulfate. Int J Mass Spectrom. 2011;305(2–3):131–7. https://doi.org/10.1016/j.ijms.2010.10.017.
16. Wolff JJ, Laremore TN, Busch AM, Linhardt RJ, Amster IJ. Electron detachment dissociation of dermatan sulfate oligosaccharides. J Am Soc Mass Spectrom. 2008;19(2):294–304. https://doi.org/10.1016/j.jasms.2007.10.007.
17. Wolff JJ, Laremore TN, Busch AM, Linhardt RJ, Amster IJ. Influence of charge state and sodium cationization on the electron detachment dissociation and infrared multiphoton dissociation of glycosaminoglycan oligosaccharides. J Am Soc Mass Spectrom. 2008;19(6):790–8. https://doi.org/10.1016/j.jasms.2008.03.010.
18. Leach FE, Xiao Z, Laremore TN, Linhardt RJ, Amster IJ. Electron detachment dissociation and infrared multiphoton dissociation of heparin tetrasaccharides. Int J Mass Spectrom. 2011;308(2):253–9. https://doi.org/10.1016/j.ijms.2011.08.029.
19. Leach FE, Wolff JJ, Laremore TN, Linhardt RJ, Amster IJ. Evaluation of the experimental parameters which control electron detachment dissociation, and their effect on the fragmentation efficiency of glycosaminoglycan carbohydrates. Int J Mass Spectrom. 2008;276(2):110–5. https://doi.org/10.1016/j.ijms.2008.05.017.
20. Leach FE 3rd, Riley NM, Westphall MS, Coon JJ, Amster IJ. Negative electron transfer dissociation sequencing of increasingly sulfated glycosaminoglycan oligosaccharides on an Orbitrap mass spectrometer. J Am Soc Mass Spectrom. 2017. https://doi.org/10.1007/s13361-017-1709-9.
21. Franklin E, Leach I, Wolff JJ, Xiao Z, Ly M, Laremore TN, et al. Negative electron transfer dissociation Fourier transform mass spectrometry of glycosaminoglycan carbohydrates. Eur J Mass Spectrom. 2011;17(2):167–76. https://doi.org/10.1255/ejms.1120.
22. Wu J, Wei J, Hogan JD, Chopra P, Joshi A, Lu W, et al. Negative electron transfer dissociation sequencing of 3-O-sulfation-containing heparan sulfate oligosaccharides. J Am Soc Mass Spectrom. 2018;29(6):1262–72. https://doi.org/10.1007/s13361-018-1907-0.
23. Huang R, Zong C, Venot A, Chiu Y, Zhou D, Boons G-J, et al. De novo sequencing of complex mixtures of heparan sulfate oligosaccharides. Anal Chem. 2016;88(10):5299–307. https://doi.org/10.1021/acs.analchem.6b00519.
24. Huang R, Pomin VH, Sharp JS. LC-MS(n) analysis of isomeric chondroitin sulfate oligosaccharides using a chemical derivatization strategy. J Am Soc Mass Spectrom. 2011;22(9):1577–87.
25. Huang R, Liu J, Sharp JS. An approach for separation and complete structural sequencing of heparin/heparan sulfate-like oligosaccharides. Anal Chem. 2013;85(12):5787–95. https://doi.org/10.1021/ac400439a.
26. Liang Q, Chopra P, Boons G-J, Sharp JS. Improved de novo sequencing of heparin/heparan sulfate oligosaccharides by propionylation of sites of sulfation. Carbohydr Res. 2018;465:16–21. https://doi.org/10.1016/j.carres.2018.06.002.
27. Lin L, Liu X, Zhang F, Chi L, Amster IJ, Leach FE, et al. Analysis of heparin oligosaccharides by capillary electrophoresis-negative-ion electrospray ionization mass spectrometry. Anal Bioanal Chem. 2017;409(2):411–20. https://doi.org/10.1007/s00216-016-9662-1.
28. Salomé P, Chrystel L-B, Jean-Claude J, Jean-Yves S, Régis D. Isomer separation and effect of the degree of polymerization on the gas-phase structure of chondroitin sulfate oligosaccharides analyzed by ion mobility and tandem mass spectrometry. Rapid Commun Mass Spectrom. 2017;31(23):2003–10. https://doi.org/10.1002/rcm.7987.
29. Renois-Predelus G, Schindler B, Compagnon I. Analysis of sulfate patterns in glycosaminoglycan oligosaccharides by MSn coupled to infrared ion spectroscopy: the case of GalNAc4S and GalNAc6S. J Am Soc Mass Spectrom. 2018;29(6):1242–9. https://doi.org/10.1007/s13361-018-1955-5.
30. Reinhold BB, Reinhold VN. Characterization of glycosylphosphatidyl-inositol (GPI) anchors by electrospray ionization and collision induced dissociation. Nippon Iyo Masu Supekutoru Gakkai Koenshu. 1992;17:117–29.
31. Redman CA, Green BN, Thomas-Oates JE, Reinhold VN, Ferguson MAJ. Analysis of glycosylphosphatidylinositol membrane anchors by electrospray ionization-mass spectrometry and collision induced dissociation. Glycoconj J. 1994;11(3):187–93. https://doi.org/10.1007/BF00731217.
32. Chan S, Reinhold VN. Detailed structural characterization of lipid A: electrospray ionization coupled with tandem mass spectrometry. Anal Biochem. 1994;218(1):63–73. https://doi.org/10.1006/abio.1994.1141.
33. Ashline DJ, Duk M, Lukasiewicz J, Reinhold VN, Lisowska E, Jaskiewicz E. The structures of glycophorin C N-glycans, a putative component of the GPC receptor site for Plasmodium falciparum EBA-140 ligand. Glycobiology. 2015;25(5):570–81. https://doi.org/10.1093/glycob/cwu188.
34. Ashline DJ, Yu Y, Lasanajak Y, Song X, Hu L, Ramani S, et al. Structural characterization by multistage mass spectrometry (MSn) of human milk glycans recognized by human rotaviruses. Mol Cell Proteomics. 2014;13(11):2961–74. https://doi.org/10.1074/mcp.M114.039925.
35. Ashline DJ, Zhang H, Reinhold VN. Isomeric complexity of glycosylation documented by MSn. Anal Bioanal Chem. 2017;409(2):439–51. https://doi.org/10.1007/s00216-016-0018-7.
36. Ashline D, Singh S, Hanneman A, Reinhold V. Congruent strategies for carbohydrate sequencing. 1. Mining structural details by MSn. Anal Chem. 2005;77(19):6250–62. https://doi.org/10.1021/ac050724z.
37. Ashline DJ, Lapadula AJ, Liu YH, Lin M, Grace M, Pramanik B, et al. Carbohydrate structural isomers analyzed by sequential mass spectrometry. Anal Chem. 2007;79(10):3830–42. https://doi.org/10.1021/ac062383a.
38. Guo Q. Development of an isotopic approach for detailing heparin sequences [Doctoral Dissertations]: University of New Hampshire; 2015.
39. Heiss C, Wang Z, Azadi P. Sodium hydroxide permethylation of heparin disaccharides. Rapid Commun Mass Spectrom. 2011;25(6):774–8. https://doi.org/10.1002/rcm.4930.
40. Anumula KR, Taylor PB. A comprehensive procedure for preparation of partially methylated alditol acetates from glycoprotein carbohydrates. Anal Biochem. 1992;203(1):101–8. https://doi.org/10.1016/0003-2697(92)90048-C.
41. Nagasawa K, Inoue Y, Kamata T. Solvolytic desulfation of glycosaminoglycuronan sulfates with dimethyl sulfoxide containing water or methanol. Carbohydr Res. 1977;58(1):47–55. https://doi.org/10.1016/S0008-6215(00)83402-3.
42. Hammad LA, Derryberry DZ, Jmeian YR, Mechref Y. Quantification of monosaccharides through multiple-reaction monitoring liquid chromatography/mass spectrometry using an aminopropyl column. Rapid Commun Mass Spectrom. 2010;24(11):1565–74. https://doi.org/10.1002/rcm.4536.
43. Stevenson TT, Furneaux RH. Chemical methods for the analysis of sulphated galactans from red algae. Carbohydr Res. 1991;210:277–98.
44. Langeslay DJ, Young RP, Beni S, Beecher CN, Mueller LJ, Larive CK. Sulfamate proton solvent exchange in heparin oligosaccharides: evidence for a persistent hydrogen bond in the antithrombin-binding pentasaccharide Arixtra. Glycobiology. 2012;22(9):1173–82. https://doi.org/10.1093/glycob/cws085.

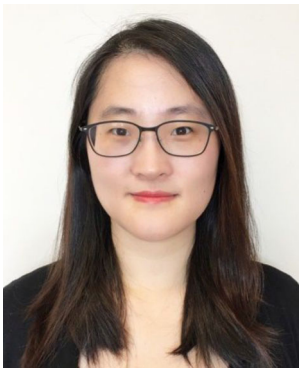

Qing Guo is a post-doctoral research scientist at the University of New Hampshire with Dr. Vernon Reinhold. Her research interest is focused on structural analysis of carbohydrates by ion trap mass spectrometry.

Vernon N. Reinhold is a Research Professor of Molecular, Cellular and Biomedical Sciences and the Director of the Glycomics Center at the University of New Hampshire. He is a pioneer in structural glycobiology and has been working in the field for over 50 years.